POLISH POLAR RESEARCH
vol. 39, no. 1, pp. 145–164, 2018 doi: 10.24425/118742

Wave characteristics and wave energy assessment in the Barents Sea

Chenglin DUAN[1], Zhifeng WANG[1,2*] and Sheng DONG[1,2]

[1] *College of Engineering, Ocean University of China, Qingdao 266100, China*

[2] *Shandong Provincial Key Laboratory of Ocean Engineering, Qingdao 266100, China*

[*] *corresponding author <wzf1984@ouc.edu.cn>*

Abstract: In this study, atlases of wave characteristics and wave energy for the Barents Sea have been generated for the years from 1996 to 2015 based on ERA-Interim datasets from the European Centre for Medium-Range Weather Forecasts (ECMWF). The wave power resources in the Barents Sea can be exploited with sea ice extent declining in recent years. The entire Barents Sea has been divided into multi-year sea ice zones, seasonal sea ice zones and open water zones according to the 20-year averaged sea ice concentration. In the entire domain, the spatial distributions of the annual averaged and mean monthly significant wave heights and wave energy flux are presented. For the open water zones, 15 points have been selected at different locations so as to derive and study the wave energy roses and the inter-annual wave power variation. Moreover, the correlations between the wave energy period and the significant wave height are shown in the energy and scatter diagrams. The maximum wave power occurs in the winter in the western parts of the Barents Sea with more than 60kW/m. The wave energy can therefore be exploited in the open water zones.

Key words: Arctic, Barents Sea, ERA-Interim, sea ice, surface waves, spatio-temporal variation.

Introduction

Recently, the exploitation of renewable energy is of great importance due to the high levels of carbon dioxide in the atmosphere. We are confronted with climate change and the shortage of the conventional energies, such as the limited fossil fuels. Various renewable and sustainable energy resources are available, such as solar, wind, hydrogen, bioenergy, ocean (*i.e.* waves, tides and currents) and geothermal energy (Saket and Etemad-Shahidi 2012; Banerjee *et al.* 2015).

Among all the renewable energy resources, wave energy is considered a rich source of renewable energy that can reduce negative impacts of fossil fuels on

the environment. Thus, detailed knowledge of wave climate is indispensable for planning and constructions of wave energy converters. In this regard, assessments of the wave energy have been studied globally (Arinaga and Cheung 2012; Gunn and Stock-Williams 2012; Zheng *et al*. 2014) and regionally in North and South of America (Beyene and Wilson 2007; Defne *et al*. 2009; Alonso *et al*. 2015; Mediavilla and Sepúlveda 2016); in Asia (Nagai *et al*. 1998; Chu and Cheng 2008; Kim *et al*. 2011; Wang *et al*. 2016); in Australia (Hughes and Heap 2010; Morim *et al*. 2016) in the Cape Verde Islands and Fiji Islands (Ram *et al*. 2014; Bernardino *et al*. 2017) and in Europe (Pontes *et al*. 1996; Sebastião *et al*. 2000; Akpınar and Kömürcü 2013; Jadidoleslam *et al*. 2016; Kalogeri *et al*. 2017). Since wave energy was first converted to electricity in France in 1799 (Clément *et al*. 2002), various wave energy converters from fixed foundations to floating substructures have been designed, which use different mechanisms to take advantage of the ocean wave fluctuations. Further, many methodologies and theories have been developed to evaluate the performance of wave energy converters (Kofoed *et al*. 2013; Rusu and Onea 2015).

The Barents Sea is located within the Arctic Circle (Fig. 1) and possesses abundant wave power as compared with other seas in the same latitudes, such as Chukotka Sea and Beaufort Sea (Arinaga and Cheung 2012). In particular, the wave energy resource in the Barents Sea can be exploited and utilized with the decline of the sea ice in recent years. Herbaut *et al*. (2015) estimated that since 2005, the ice area in the Barents Sea has decreased rapidly, reaching a mean of 400 000 km^2 from 670 000 km^2 over the period 2005–2012. The rapid plummet of the ice area is probably related to the oceanic heat transport governed by wind-driven Atlantic water flow (Lien *et al*. 2017). Shapiro *et al*. (2003) found that the mean ice edge retreated north-eastward and the most spectacular ice edge retreat was between 25°E and 49°E longitude. Therefore, wave energy can be exploited and developed in the ice-free zones of the Barents Sea. Based on the European Centre for Medium-Range Weather Forecasts (ECMWF) ERA-40 datasets for the period between September 1957 and August 2002, Reistad *et al*. (2011) used the dynamic atmospheric downscaling and the nested WAM wave model to obtain a hindcast of wind and wave in the Barents Sea. Using hindcast datasets from the Norwegian Reanalysis 10 km database, Orimolade *et al*. (2016) estimated the extreme significant wave heights and the associated uncertainties in the western Barents Sea. However, the aforementioned studies did not fully focus on the wave behaviors in the Barents Sea. Consequently, there is insufficient information on the wave characteristics to enable an assessment of the wave energy for engineering purposes.

The main objective of this study is to analyze the datasets from ECMWF ERA-Interim to determine the wave climate, the available seasonal and annual averaged wave power density in the Barents Sea. There are four sections in this paper. The study area, introduction of data from ECMWF ERA-Interim and the

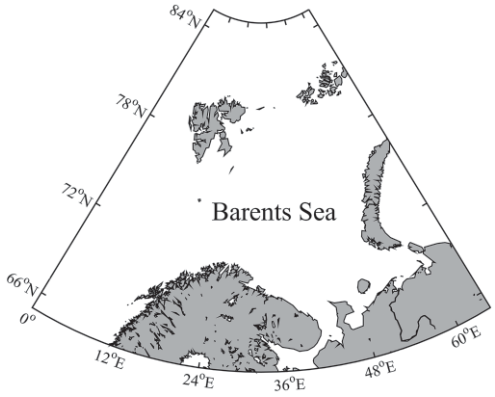

Fig. 1. The location of the study area.

methodology for evaluating the wave behaviors and power density are described in *Materials and methodology* section. The results and discussions of the wave characteristics and wave energy are presented in *Results and interpretations* section. Finally, summary and conclusions are shown in *Conclusions* section.

Materials and methodology

Study area and data description. — Based on the earlier studies on the Barents Sea (Lien *et al*. 2017), the area covering 65°N to 85°N and 0°E to 65°E has been analyzed in this study (Fig. 1). The data used for the estimation and analysis is derived from the ERA-Interim datasets, which has been generated from the large hindcast projects by the well-known ECMWF. Many studies used these datasets to perform similar assessments and analyses (Musić and Nicković 2008; Reistad *et al*. 2011). In this study, the data between 1996 and 2015 with a temporal resolution of 6 h and a spatial resolution of 0.125° by 0.125° have been selected. The values of the wave parameters, such as significant height of combined wind waves and swell, mean wave period and mean wave direction, have been given. Moreover, in order to determine the ice-free extent in the Barents Sea, the datasets of the sea ice have been taken into consideration. The sea ice concentration is selected which is represented by the sea-ice cover in the ERA-Interim.

Methods of calculating sea ice. — The fraction of ice relative to the total area at a given grid in the ocean is the sea ice concentration, from which ice extent, ice area and area of open water within the ice pack can be calculated (Comiso *et al*. 1997). The sea ice extent is determined by suming up the area of all the grid cells in the Barents Sea with at least 15% of sea ice. The calculating equation can be expressed as (Ogi *et al*. 2008):

$$SIE = \sum_{i=1}^{n} w_i A_i = \begin{cases} w_i = 1, a_i \geq 15\% \\ w_i = 0, a_i < 15\% \end{cases} \quad (1)$$

where SIE is the sea ice extent, A_i is the area of that grid, a_i is the sea ice concentration, and w_i is the weight coefficient.

Methods of calculating wave energy. — The main wave characteristics parameters are significant wave height, H_s, and mean wave period, T_m. Both H_s and T_m can be directly obtained from the ERA-Interim datasets while the wave power is calculated by following equations (2–4). In deep water areas, the wave energy, defined as the flux per unit width of the progressing wave front in terms of the H_s and T_m, is (Tucker and Pitt 2001; Akpınar and Kömürcü 2013):

$$E_k = \frac{\rho g^2}{64\pi} T_e H_s^2 \quad (2)$$

where ϱ and g are the seawater density and gravitational acceleration respectively; and T_e is the energy period, representing the period of a sinusoidal wave within the same energy content of the sea condition.

The relationship among the energy period, T_e, the peak period, T_p, and the mean period, T_m, can be expressed as follows (Boccotti 2014):

$$T_e = \lambda T_p \quad (3)$$

$$T_m = \xi T_p \quad (4)$$

For JONSWAP spectrum, conversion coefficients λ and ξ equal to 0.9 and 0.78 respectively when the spectral peak enhancement factor γ equals to 3.3.

Results and interpretations

Evaluation of sea ice distribution. — As the Barents Sea is largely covered with ice, the wave propagation and height is inevitably hindered especially in the northern sea zones. Using equation (1), the mean monthly and annual averaged sea ice extent have been determined. Averaged sea ice extent reaches the largest in April and then decreases to the smallest in September (Fig. 2). Meanwhile, the ice edge undergoes seasonal advance and retreat. Therefore, the entire Barents Sea can be divided into multi-annual sea ice zones, seasonal sea ice zones and open water zones. In the seasonal ice zones, the first-year ice exists. In the open water zones, (*i.e.* the ice-free area), there is almost no drift or floating ice. The three different zones and two relevant ice edge lines are shown in Figure 3.

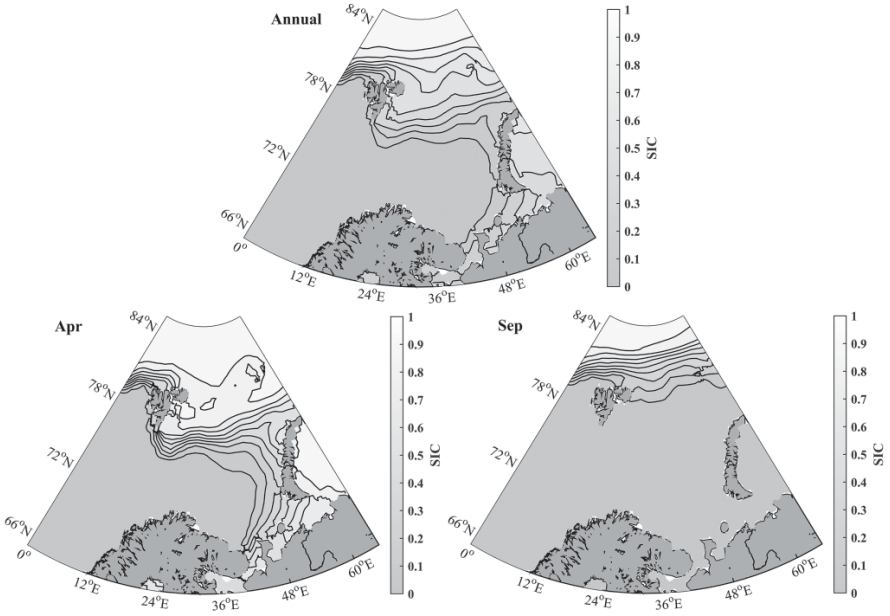

Fig. 2. Averaged annual, monthly maximum (April), and minimum (September) distribution of sea ice concentrations (SIC).

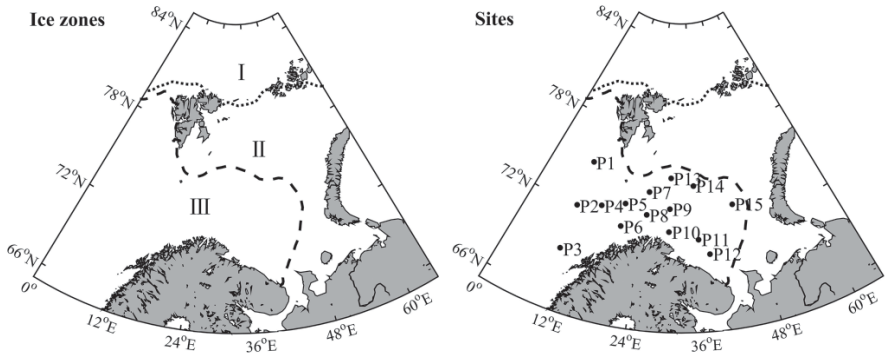

Fig. 3. Divided ice zones in the study area; zones I, II and III are the multi-annual sea ice zones, seasonal sea ice zones and open water zones, respectively. The two stippled lines are the mean sea ice edges in September and April, respectively; in zone III, locations of selected points in the domain are shown for further wave energy assessment.

Evaluation of annual wave climate and energy. — By averaging the 20 years ERA-Interim datasets, the mean significant wave height, H_s, and wave power density, E_k, in the Barents Sea have been calculated. Figure 4 shows the average annual spatial distribution maps H_s of and E_k in the pattern of a contour map.

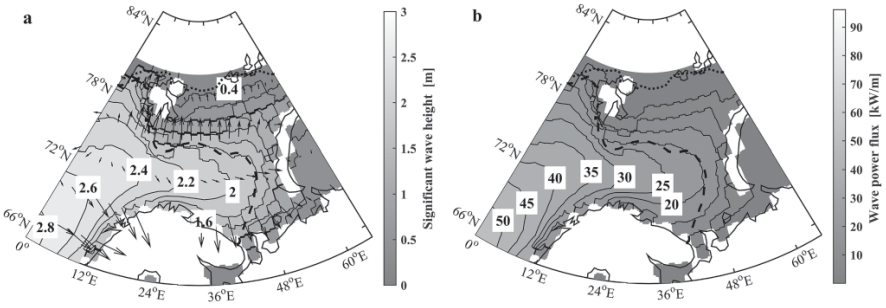

Fig. 4. Spatial distributions of mean annual averaged significant wave height (**a**) and wave energy flux (**b**).

The waves with significant wave heights between 0 m and 2.8 m with 0–50 kW/m wave power flux are present in most parts of the entire domain. The waves with larger significant wave heights are mostly in the western part of the Barents Sea, where the wave power is greater than 35 kW/m. In the eastern parts of the Barents Sea, (*i.e.* between 50°E and 65°E longitude), there are no strong waves and, consequently, the wave power is lower. The gradual decreasing trends of both H_s and E_k from west to east are due to the variations of the powerful swell, which comes from Norwegian Sea (Reistad *et al.* 2011). Further, in the coastal zones the wave power density and significant wave height are relatively low. This is probably on account of wave dissipation due to depths variation effects. In the seasonal sea ice zones, the waves with significant wave height and wave energy less than 1.8 m and 20 kW/m, respectively, are weaker than those in open sea water zones due to the existence of ice and less energetic swell. Hence, the waves in the open water zones may be exploited for wave energy.

Evaluation of mean monthly wave climate and energy. — Generally, wave climate and stored wave power potential are closely related to the weather conditions. In other words, the wave conditions may change from year to year, month to month and day to day. Therefore, monthly analysis is important for a detailed understanding of the temporal variations of the waves in the domain. Using the average data of the same month in each year from 1996 to 2015, the mean monthly spatial atlases of significant wave height and wave power capacity have been derived.

Figures 5–8 shows the mean monthly spatial distributions of the significant wave height and wave power flux in each month. From the figures, the most powerful waves are in the western parts of the domain throughout the years but have different wave states and power potential in different months. In the winter (*i.e.* December, January, February), the significant wave heights are between 2.4 m

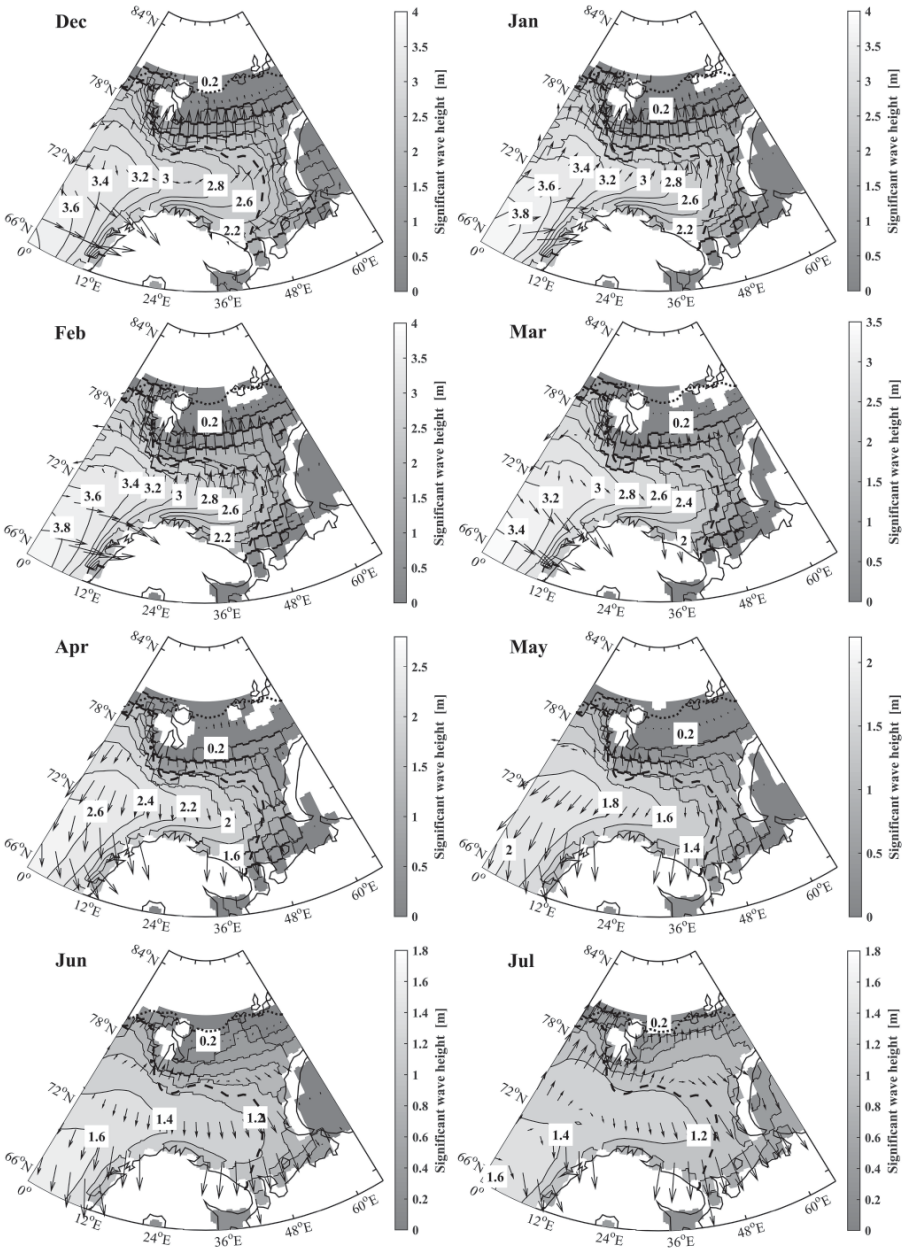

Fig. 5. Spatial distributions of mean monthly significant wave height from December to July.

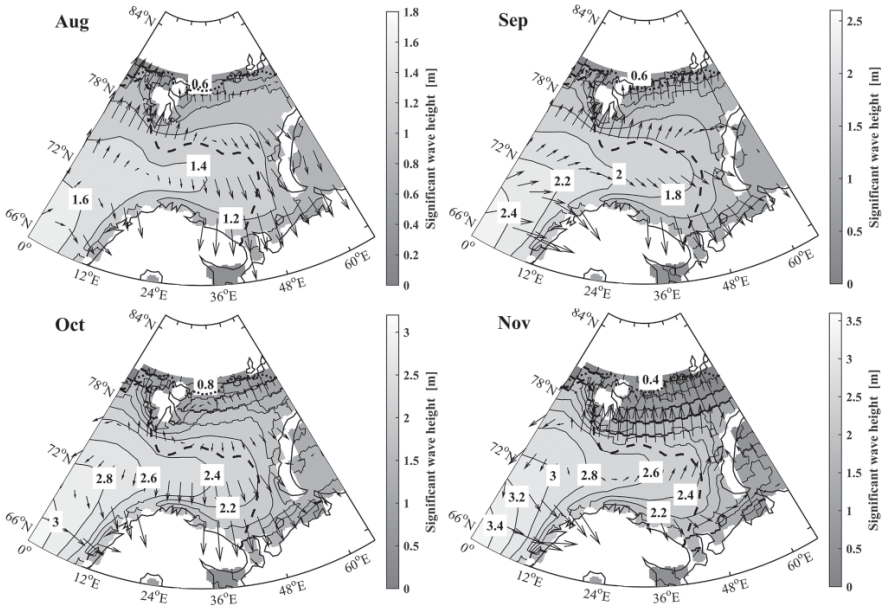

Fig. 6. Spatial distributions of mean monthly significant wave height from August to November.

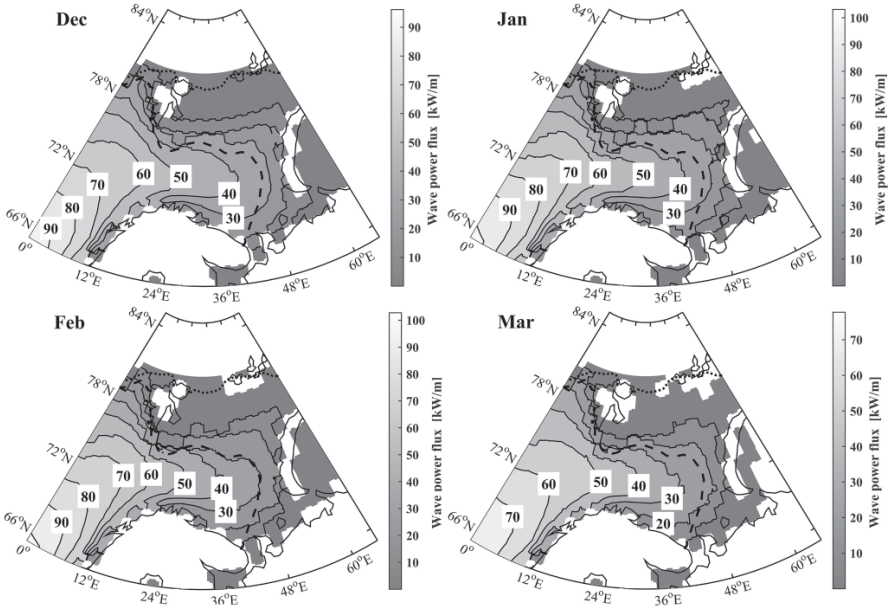

Fig. 7. Spatial distributions of mean monthly wave power flux from December to March.

and 3.8 m with wave energy flux between 30 kW/m and 90 kW/m in the open sea water zones. In the summer (*i.e.* June, July, August), the significant wave heights and wave energy flux are at their lowest with no more than 1.7 m and 14 kW/m in the same zones. According to the 20-year wave analysis, July is the calmest month among the 12 months in a year. March and November are the two months with higher significant wave heights (> 3 m) and larger wave power (> 60 kW/m) in the western Barents Sea. During the other months, the significant wave height and wave power are with intermediate. In the seasonal sea ice zones, the significant wave height is less than 2 m throughout the year. It is noticeable that the significant wave height and wave energy density vary with season.

Evaluation of wave energy roses. — The wave directions are also highly dependent on the weather conditions. Hence, the wave directions change yearly, seasonally, monthly or even daily. Therefore, in order to have a better understanding of the wave behaviors, it is important to study directional distributions of the wave power density in different sea areas. In this regard, various points have been selected in such a way that all the whole open sea water zones are covered. Figure 3 shows the geographical locations of the points and the points have been labeled from P1 to P15. Points from P13 to P15 are near the sea ice marginal zones and the other points are in the area where there was no sea ice for twenty years. The mean significant wave height and mean wave period at these points are between 1.78 m and 2.53 m, and between 6.55 s and 8.30 s, respectively (Table 1).

Based on the 20-year datasets, the wave energy roses at the selected 15 points are shown in figures 9 and 10. In this study, wave potential has been separated into seven intervals from 0 to > 60 kW/m. According to the wave roses, the dominant wave directions are different at different locations. The dominant wave direction is SW in the western parts of the domain (*i.e.* P1, P2, P3, P4, P5). The dominant wave directions are WSW and W in the central part of the open sea water zones (*i.e.* P6, P7, P8, P9). In the southeastern parts (*i.e.* P10, P11, P12), NW, NNW, N and NNE waves contribute most for the wave energy potential. In the near sea ice marginal zones (*i.e.* P13, P14, P15), W, WSW, N are the recurring wave directions. The results of this analysis are important because the wave energy converters can then be installed in the energetic wave directions.

Evaluation of correlations between wave energy period and significant wave height. — In order to find out the composition of the wave energy resources in terms of the significant wave height and energy period, the combined scatter and energy diagrams at all 15 points have been prepared (Figs. 11–13). These diagrams represent the occurrence of various classified sea conditions according to their energy period, significant wave height and their contribution to the total annual wave power with reference to the average year, which is the average

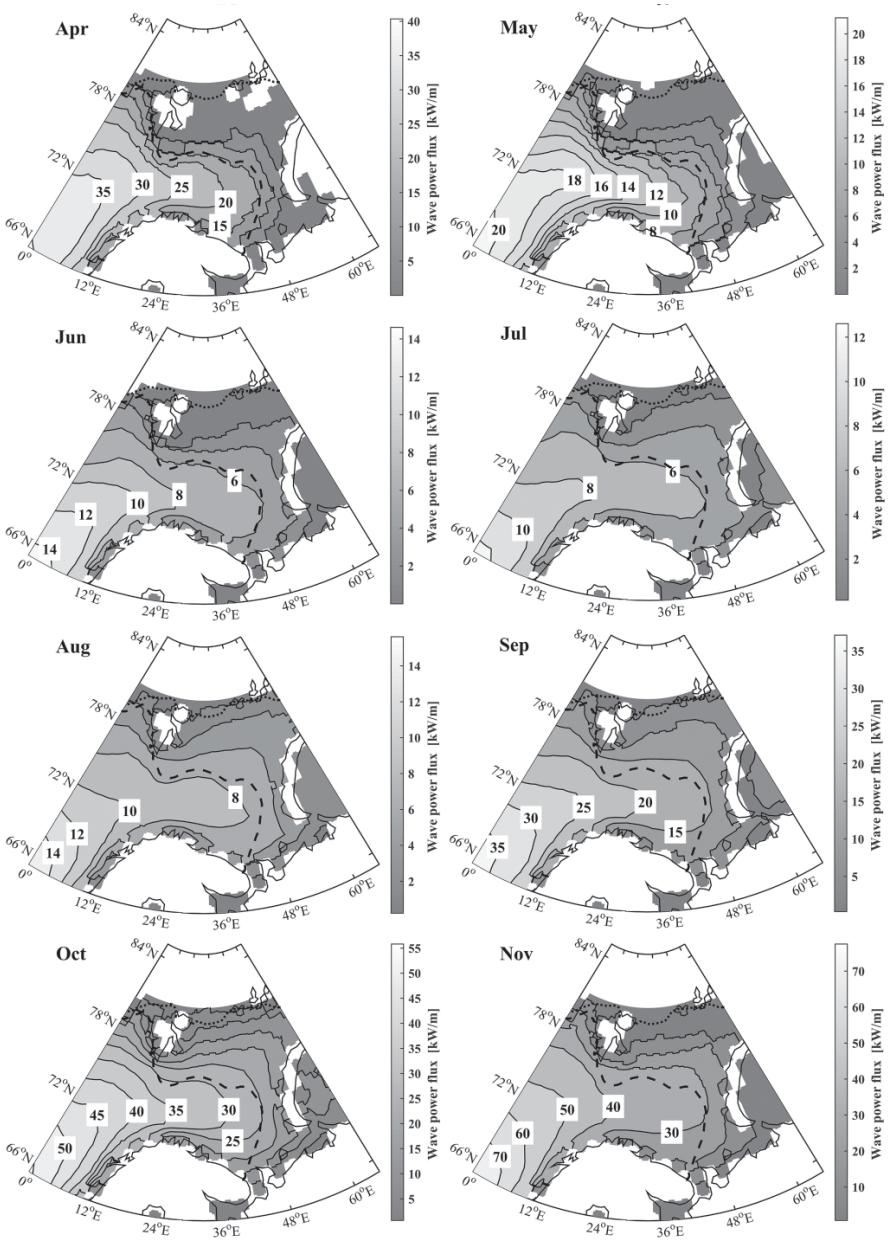

Fig. 8. Spatial distributions of mean monthly wave power flux (kW/m) from April to November.

Table 1

Locations of selected points and mean significant wave height $\bar{H}_s$ and mean wave period $\bar{T}$ at each point; the minimum and maximum of each parameter are indicated with a single underline and a double underline, respectively.

Point	Longitude	Latitude	$\bar{H}_s$ [m]	$\bar{T}$ [s]
P1	10	75	2.32	7.72
P2	10	72	2.53	8.09
P3	10	69	2.50	8.30
P4	15	72.5	2.44	7.98
P5	20	73	2.34	7.85
P6	20	71.5	2.19	7.89
P7	25	74	2.21	7.60
P8	25	72.5	2.23	7.67
P9	30	73	2.20	7.52
P10	30	71.5	1.94	7.08
P11	36	71	1.91	6.80
P12	38	70	1.78	6.55
P13	30	75	2.06	7.29
P14	34.5	74.5	2.02	7.16
P15	44	73	1.94	7.01

of the 20 years in the ERA-Interim datasets. With the correlations and using the approaches introduced by Dunnett and Wallace (2009), we can ensure the better performances of the wave energy converters.

The area within the combined energy and scatter diagrams is separated into virtual squares of 1 m and 1 s. The number in each square is the occurrence of that sea conditions in number of hours per year whose energy period and significant wave height are just in corresponding range. The small numbers in the upper part of the diagrams represent the low likelihood of waves with high height.

The range of the energy periods is very wide in the open sea water zones (Figs. 11–13). Most of the wave power is supplied by the significant wave heights between 0 m and 12 m and the energy periods between 3 s and 17 s. The majority of the wave power density is offered by the significant wave heights between 1 m and 6 m and the periods between 7 s and 12 s in the Barents Sea.

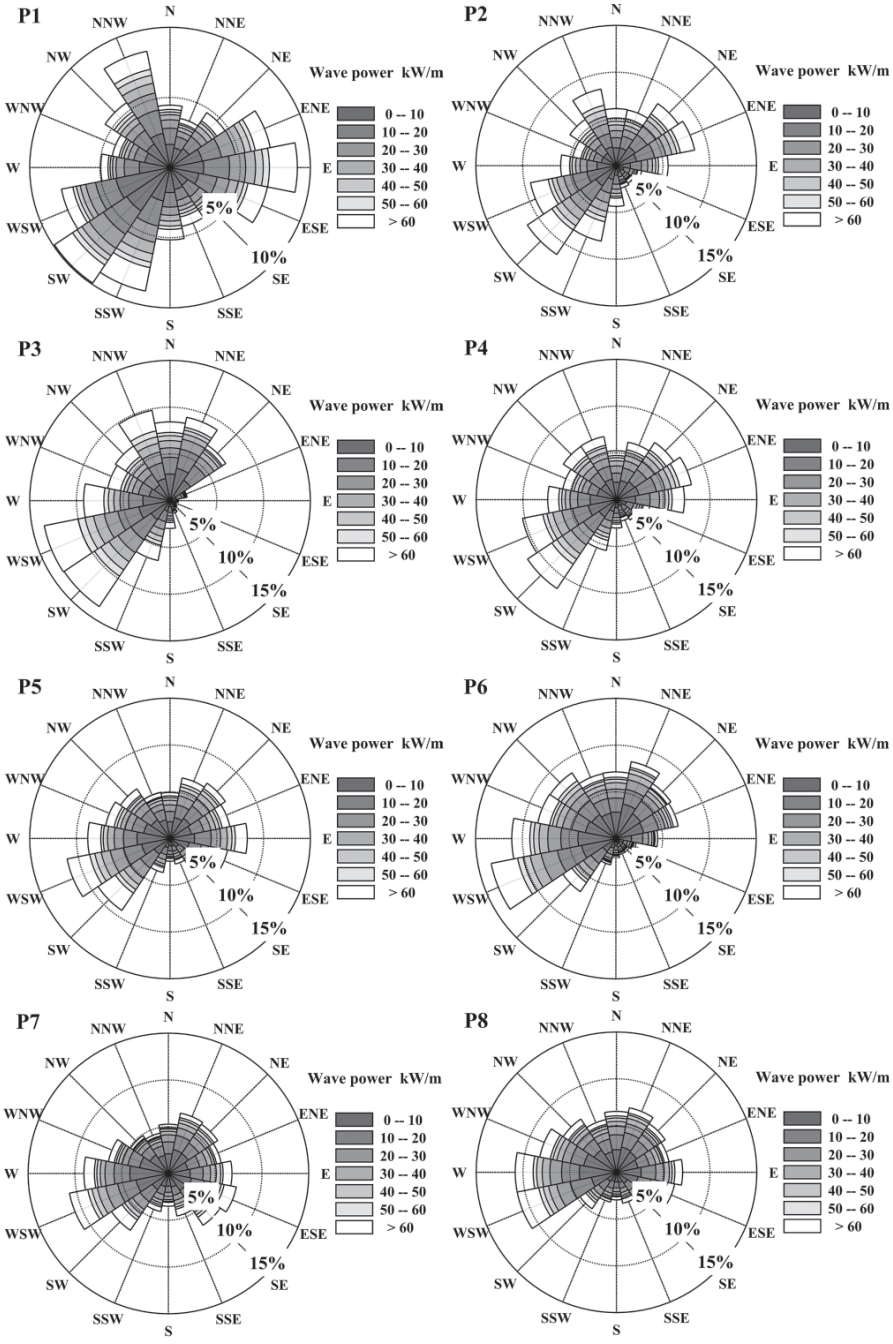

Fig. 9. Wave energy roses for sites P1 to P8.

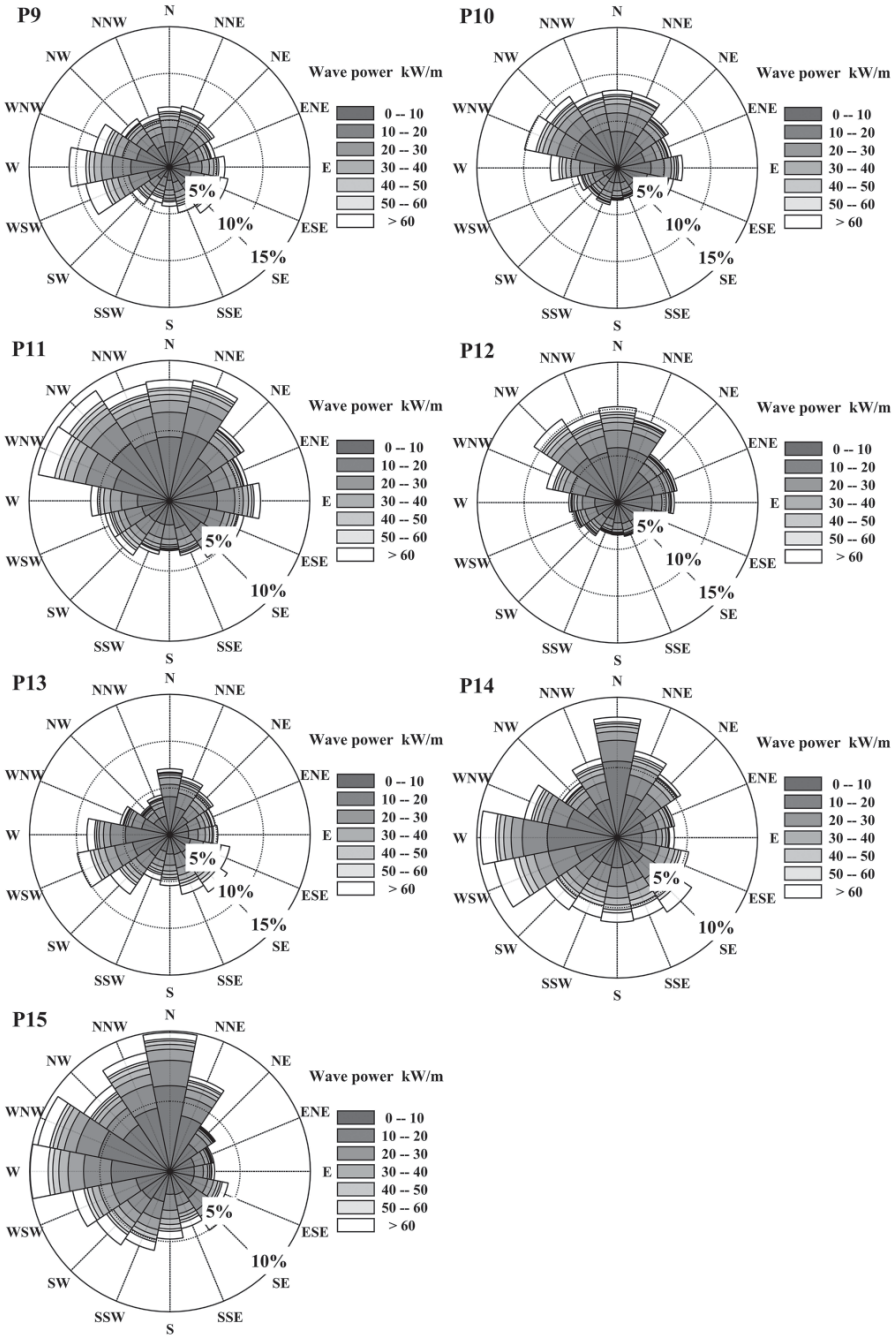

Fig. 10. Wave energy roses for sites P9 to P15.

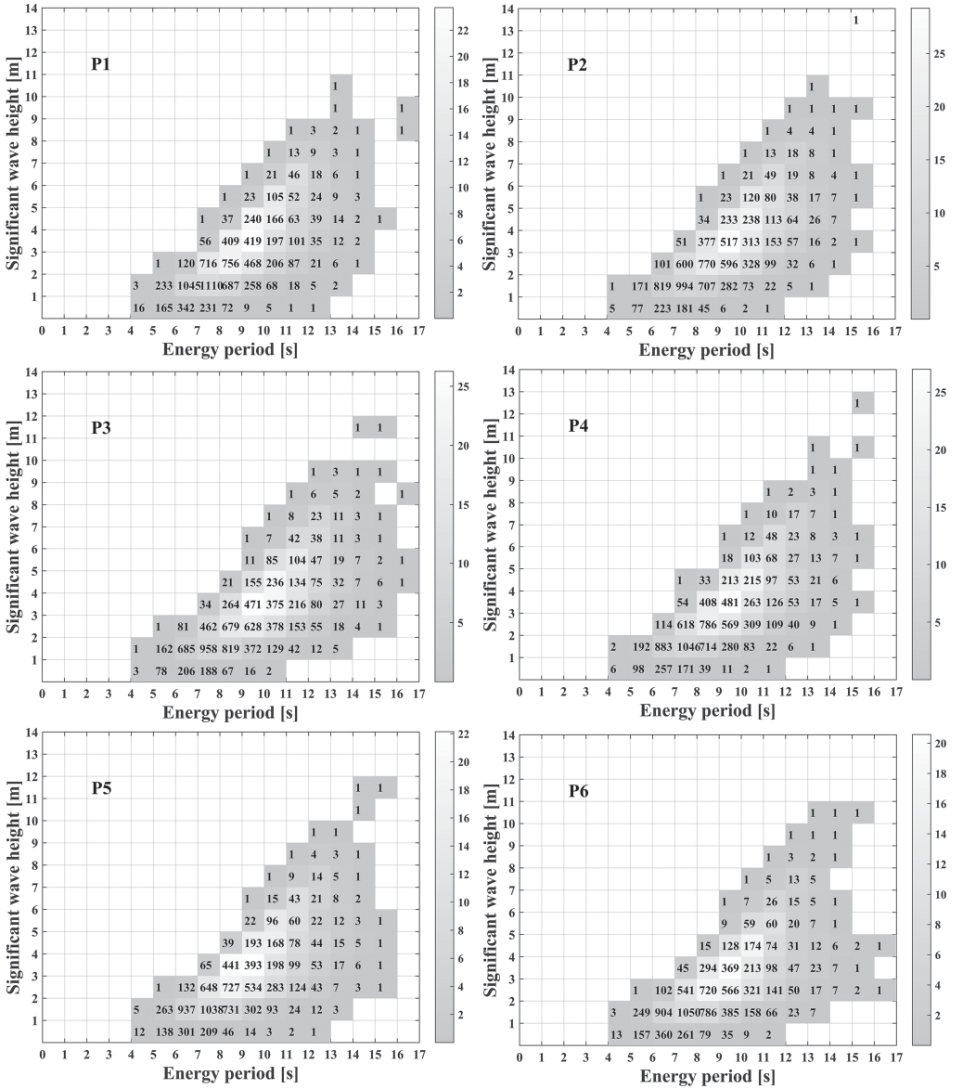

Fig. 11. Combined energy and scatter diagrams of the annual energy corresponding to sea conditions of T_e and H_s from P1 to P6; the numbers indicate the occurrence of sea conditions in number of hours per year and the grey tonal scale represents total annual energy per meter of wave front in MWh/m.

Evaluation of interannual variation of average wave energy. — To make clear the interannual variations of wave power density is also required to access more detailed analysis. Figure 14 shows the continuous temporal variation of the average wave power density at the 15 selected points from 1996 to 2015. It can be seen that at most points, the average wave power density is similar

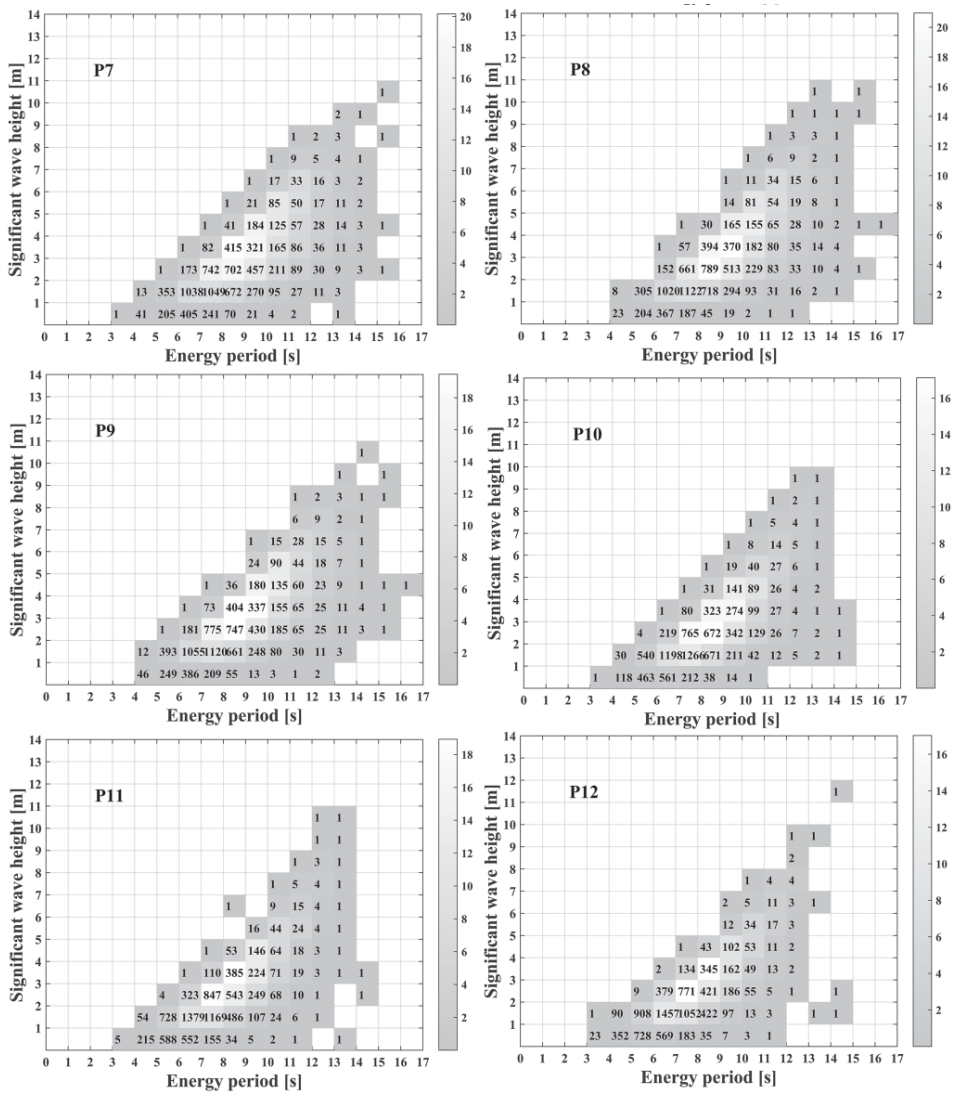

Fig. 12. Combined energy and scatter diagrams of the annual energy corresponding to sea conditions of T_e and H_s from P7 to P12; the numbers indicate the occurrence of sea conditions in number of hours per year and the grey tonal scale represents total annual energy per meter of wave front in MWh/m.

within a variation range of 5 kW/m, except in 1997, 2006, 2011 and 2015 when the density is relatively higher. Further, it is also obvious that the wave energy density is higher in the western Barents Sea than that in the eastern Barents Sea and it is stronger in the offshore area than that in the coastal zones.

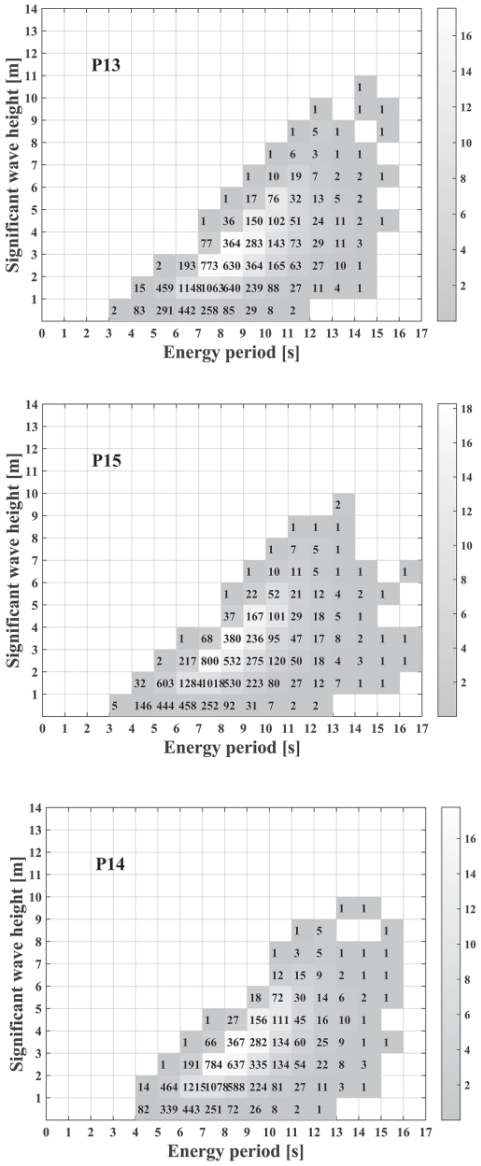

Fig. 13. Combined energy and scatter diagrams of the annual energy corresponding to sea conditions of T_e and H_s from P13 to P15; the numbers indicate the occurrence of sea conditions in number of hours per year and the grey tonal scale represents total annual energy per meter of wave front in MWh/m.

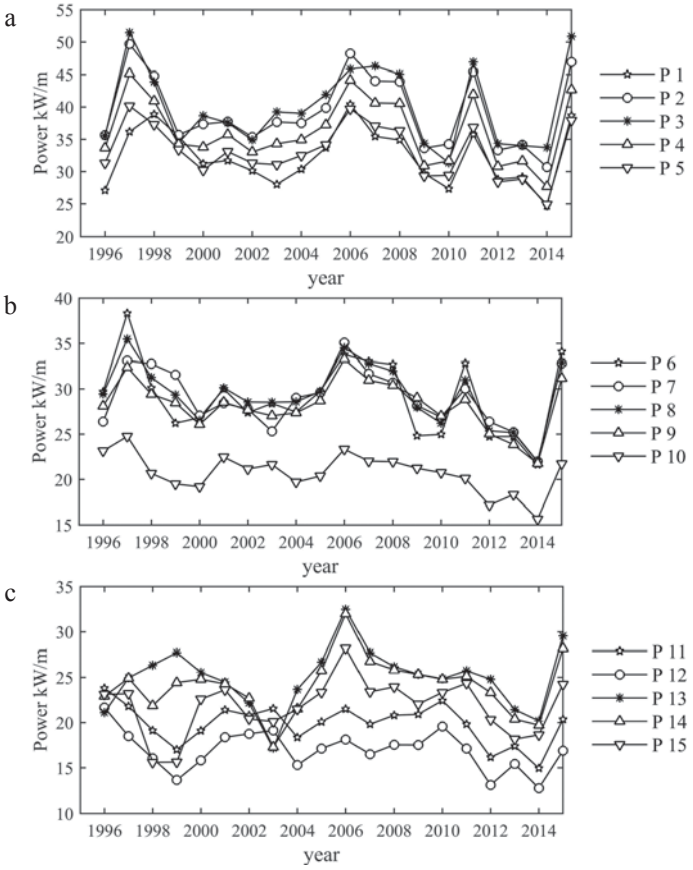

Fig. 14. Interannual variation of mean annual averaged wave power flux in kW/m at selected 15 points, P1 to P5 (**a**), P6 to P10 (**b**) and P11 to P15 (**c**), from 1996 to 2015.

Conclusions

In the Barents Sea, due to the oceanic heat transport and global warming in recent years, the ice is increasingly declining. The entire Barents Sea can be divided into multi-year sea ice zones, seasonal sea ice zones and open sea water zones according to the mean monthly sea ice concentration. Therefore the wave energy resources in the open sea water zones can be exploited and utilized as a renewable and sustainable resource.

The spatial and temporal analysis of the wave climate and energy power has been carried out in detail. Results show that waves offshore are generally stronger than those nearshore and in sea ice zones. The larger wave heights are more frequent in the western parts of the Barents Sea, where the annual averaged wave

power exceeds 35 kW/m and sometimes even more than 60 kW/m. The mean wave power potential has the maximum in winter months with the significant wave heights between 2.4 m and 3.8 m and wave energy flux between 30 kW/m and 90 kW/m in the open sea water zones. Further, the significant wave height and wave energy density have obvious seasonal variations. In the winter, the significant wave heights and the wave energy flux reach up to the maximum, while in the summer both the significant wave heights and the wave energy flux are at their minimum. The dominant wave directions are different at different locations. The dominant wave direction is SW in the western parts of the domain, where the waves are most powerful. The majority of wave power density is provided by the significant wave heights between 1 m and 6 m and the energy periods between 7 s and 12 s in the open sea water zones. Furthermore, at most points the average wave power density is similar within a variation range of 5 kW/m.

In summary, this paper promotes the understanding of the wave characteristics in the Barents Sea and presents a statistical assessment of the wave energy resource with the ECMWF ERA-Interim datasets from 1996 to 2015.

Acknowledgements. — The authors are thankful to the reviewer Stanislaw Massel for the valuable comments and suggestions that helped to improve this paper. This work is financially supported by the National Key R&D Program of China (No. 2016YFC0303401) and National Natural Science Foundation of China (No. 51509226, 51779236).

References

AKPINAR A. and KÖMÜRCÜ M.İ. 2013. Assessment of wave energy resource of the Black Sea based on 15-year numerical hindcast data. *Applied Energy* 101: 502–512.

ALONSO R., SOLARI S. and TEIXEIRA L. 2015. Wave energy resource assessment in Uruguay. *Energy* 93: 683–696.

ARINAGA R.A. and CHEUNG K.F. 2012. Atlas of global wave energy from 10 years of reanalysis and hindcast data. *Renewable Energy* 39: 49–64.

BANERJEE S., MUSA M.N., ABU D.I.R., JAAFAR B. and ARRIFIN A. 2015. Application on solar, wind and hydrogen energy—a feasibility review for an optimised hybrid renewable energy system. *Journal of Fundamentals of Renewable Energy & Applications* 5: 193. doi:10.4172/20904541.1000193.

BERNARDINO M., RUSU L. and SOARES C.G. 2017. Evaluation of the wave energy resources in the Cape Verde Islands. *Renewable Energy* 101: 316–326.

BEYENE A. and WILSON J.H. 2007. Digital mapping of California wave energy resource. *International Journal of Energy Research* 31: 1156–1168.

BOCCOTTI P. 2014. *Wave mechanics and wave loads on marine structures*. Butterworth-Heinemann. Amsterdam: 70 pp.

CHU P.C. and CHENG K.F. 2008. South China Sea wave characteristics during Typhoon Muifa passage in winter 2004. *Journal of Oceanography* 64: 1–21.

CLÉMENT A., MCCULLEN P., FALCÃO A., FIORENTINO A., GARDNER F., HAMMARLUND K., LEMONIS G., LEWIS T., NIELSEN K., PETRONCINI S., PONTES M.T., SCHILD P., SJÖSTRÖM B.O., SØRENSEN H.C. and THORPE T. 2002. Wave energy in Europe: current status and perspectives. *Renewable and Sustainable Energy Reviews* 6: 405–431.

COMISO J.C., CAVALIERI D.J., PARKINSON C.L. and GLOERSEN P. 1997. Passive microwave algorithms for sea ice concentration: A comparison of two techniques. *Remote Sensing of Environment* 60: 357–384.

DEFNE Z., HAAS K.A. and FRITZ H.M. 2009. Wave power potential along the Atlantic coast of the southeastern USA. *Renewable Energy* 34: 2197–2205.

DUNNETT D. and WALLACE J.S. 2009. Electricity generation from wave power in Canada. *Renewable Energy* 34: 179–195.

HERBAUT C., HOUSSAIS M.N., CLOSE S. and BLAIZOT A.C. 2015. Two wind-driven modes of winter sea ice variability in the Barents Sea. *Deep Sea Research Part I: Oceanographic Research Papers* 106: 97–115.

HUGHES M.G. and HEAP A.D. 2010. National-scale wave energy resource assessment for Australia. *Renewable Energy* 35: 1783–1791.

JADIDOLESLAM N., ÖZGE M. and AĞIRALIOĞLU N. 2016. Wave power potential assessment of Aegean Sea with an integrated 15-year data. *Renewable Energy 86*: 1045–1059.

GUNN K. and STOCK-WILLIAMS C. 2012. Quantifying the global wave power resource. *Renewable Energy* 44: 296–304.

KALOGERI C., GALANIS G., SPYROU C., DIAMANTIS D., BALADIMA F., KOUKOULA M. and KALLOS G. 2017. Assessing the European offshore wind and wave energy resource for combined exploitation. *Renewable Energy* 101: 244–264.

KIM G., JEONG W.M., LEE K.S., JUN K. and LEE M.E. 2011. Offshore and nearshore wave energy assessment around the Korean Peninsula. *Energy* 36: 1460–1469.

KOFOED J.P., PECHER A., MARGHERITINI L., ANTONISHEN M., BITTENCOURT C., HOLMES B., RETZLER C., BERTHELSEN K., CROM I.LE., NEUMANN F., JOHNSTONE C., MCCOMBESJ T. and MYERS L.E. 2013. A methodology for equitable performance assessment and presentation of wave energy converters based on sea trials. *Renewable Energy* 52: 99–110.

LIEN V.S., SCHLICHTHOLZ P., SKAGSETH Ø. and VIKEBØ F.B. 2017. Wind-driven Atlantic water flow as a direct mode for reduced Barents Sea ice cover. *Journal of Climate* 30: 803–812.

MEDIAVILLA D.G. and SEPÚLVEDA H.H. 2016. Nearshore assessment of wave energy resources in central Chile (2009–2010). *Renewable Energy* 90: 136–144.

MORIM J., CARTWRIGHT N., ETEMAD-SHAHIDI A., STRAUSS D. and HEMER M. 2016. Wave energy resource assessment along the Southeast coast of Australia on the basis of a 31-year hindcast. *Applied Energy* 184: 276–297.

MUSIĆ S. and NICKOVIĆ S. 2008. 44-year wave hindcast for the Eastern Mediterranean. *Coastal Engineering* 55: 872–880.

NAGAI K., KONO S. and QUANG D.X. 1998. Wave characteristics on the central coast of Vietnam in the South China Sea. *Coastal Engineering Journal* 40: 347–366.

OGI M., RIGOR I.G., MCPHEE M.G. and WALLACE J.M. 2008. Summer retreat of Arctic Sea ice: role of summer winds. *Geophysical Research Letters* 35: 101–106.

ORIMOLADE A.P., HAVER S. and GUDMESTAD O.T. 2016. Estimation of extreme significant wave heights and the associated uncertainties: A case study using NORA10 hindcast data for the Barents Sea. *Marine Structures* 49: 1–17.

PONTES M.T., ATHANASSOULIS G.A., BARSTOW S., CAVALERI L., HOLMES B., MOLLISON D. and OLIVEIRA-PIRES, H. 1996. An atlas of the wave-energy resource in Europe. *Transactions of the ASME-O-Journal of Offshore Mechanics and Arctic Engineering* 118: 307–308.

RAM K., NARAYAN S., AHMED M.R., NAKAVULEVU P. and LEE Y.H. 2014. In situ near-shore wave resource assessment in the Fiji Islands. *Energy for Sustainable Development* 23: 170–178.

REISTAD M., BREIVIK Ø., HAAKENSTAD H., AARNES O.J., FUREVIK B.R. and BIDLOT J.R. 2011. A high-resolution hindcast of wind and waves for the North Sea, the Norwegian Sea, and the Barents Sea. *Journal of Geophysical Research: Oceans* 116: doi: 10.1029/2010JC006402

RUSU L. and ONEA F. 2015. Assessment of the performances of various wave energy converters along the European continental coasts. *Energy* 82: 889–904.

SAKET A. and ETEMAD-SHAHIDI A. 2012. Wave energy potential along the northern coasts of the Gulf of Oman, Iran. *Renewable Energy* 40: 90–97.

SEBASTIÃO P.G.S.C., SOARES C.G. and BOOIJ N. 2000. Wave hindcasting off the coast of Portugal. *Coastal engineering* 40: 411–425.

SHAPIRO I., COLONY R. and VINJE T. 2003. April sea ice extent in the Barents Sea, 1850–2001. *Polar Research* 22: 5–10.

TUCKER M.J. and PITT E.G. 2001. *Waves in ocean engineering*. Elsevier Science, New York: 521 pp.

WANG Z., DONG S., LI X. and SOARES C.G. 2016. Assessments of wave energy in the Bohai Sea, China. *Renewable Energy* 90: 145–156.

ZHENG C., SHAO L., SHI W., SU Q., LIN G., LI X. and CHEN X. 2014. An assessment of global ocean wave energy resources over the last 45 a. *Acta Oceanologica Sinica* 33: 92–101.

Received 6 April 2017
Accepted 8 January 2018